

**Modifications of gallium phosphide single crystals using slow highly charged ions and swift heavy ions**

El-Said, A. S.; Wilhelm, R. A.; Heller, R.; Akhmadaliev, S.; Schumann, E.; Sorokin, M.; Facsko, S.; Trautmann, C.;

Originally published:

May 2016

**Nuclear Instruments and Methods in Physics Research B 382(2016), 86-90**

DOI: <https://doi.org/10.1016/j.nimb.2016.04.058>

Perma-Link to Publication Repository of HZDR:

<https://www.hzdr.de/publications/Publ-23035>

Release of the secondary publication  
on the basis of the German Copyright Law § 38 Section 4.

CC BY-NC-ND

## Accepted Manuscript

Modifications of gallium phosphide single crystals using slow highly charged ions and swift heavy ions

A.S. El-Said, R.A. Wilhelm, R. Heller, Sh. Akhmadaliev, E. Schumann, M. Sorokin, S. Fascko, C. Trautmann

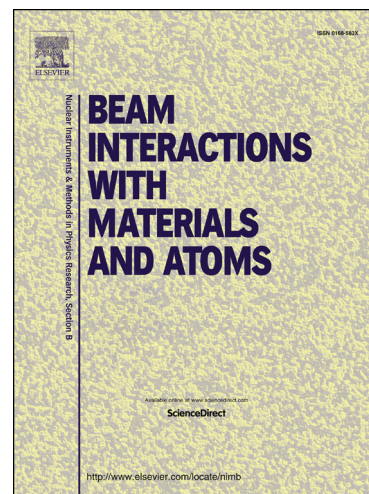
PII: S0168-583X(16)30194-X  
DOI: <http://dx.doi.org/10.1016/j.nimb.2016.04.058>  
Reference: NIMB 61868

To appear in: *Nucl. Instr. and Meth. in Phys. Res. B*

Received Date: 13 January 2016  
Revised Date: 28 April 2016  
Accepted Date: 28 April 2016

Please cite this article as: A.S. El-Said, R.A. Wilhelm, R. Heller, Sh. Akhmadaliev, E. Schumann, M. Sorokin, S. Fascko, C. Trautmann, Modifications of gallium phosphide single crystals using slow highly charged ions and swift heavy ions, *Nucl. Instr. and Meth. in Phys. Res. B* (2016), doi: <http://dx.doi.org/10.1016/j.nimb.2016.04.058>

This is a PDF file of an unedited manuscript that has been accepted for publication. As a service to our customers we are providing this early version of the manuscript. The manuscript will undergo copyediting, typesetting, and review of the resulting proof before it is published in its final form. Please note that during the production process errors may be discovered which could affect the content, and all legal disclaimers that apply to the journal pertain.



## Modifications of gallium phosphide single crystals using slow highly charged ions and swift heavy ions

A.S. El-Said<sup>1</sup>, R.A. Wilhelm<sup>2</sup>, R. Heller<sup>2</sup>, Sh. Akhmadaliev<sup>2</sup>, E. Schumann<sup>2</sup>, M. Sorokin<sup>3</sup>, S. Fascko<sup>2</sup> and C. Trautmann<sup>4,5</sup>

<sup>1</sup>Physics Department, King Fahd University of Petroleum and Minerals,  
Dhahran 31261, Saudi Arabia

<sup>2</sup>Institute of Ion Beam Physics and Materials Research, Helmholtz-Zentrum  
Dresden-Rossendorf, 01328 Dresden, Germany

<sup>3</sup>National Research Centre 'Kurchatov Institute', Kurchatov Square 1,  
123182 Moscow, Russia

<sup>4</sup>GSI Helmholtz Centre for Heavy Ion Research, 64291 Darmstadt, Germany

<sup>5</sup>Technische Universität Darmstadt, 64289 Darmstadt, Germany

### Abstract

GaP single crystals were irradiated with slow highly charged ions (HCI) using 114 keV  $^{129}\text{Xe}^{(33-40)+}$  and with various swift heavy ions (SHI) of 30 MeV  $\text{I}^{9+}$  and 374 MeV - 2.2 GeV  $^{197}\text{Au}^{25+}$ . The irradiated surfaces were investigated by scanning force microscopy (SFM). The irradiations with SHI lead to nanohillocks protruding from the GaP surfaces, whereas no changes of the surface topography were observed after the irradiation with HCI. This result indicates that a potential energy above 38.5 keV is required for surface nanostructuring of GaP. In addition, strong coloration of the GaP crystals was observed after irradiation with SHI. The effect was stronger for higher energies. This was confirmed by measuring an increased extinction coefficient in the visible light region.

Key words: GaP, swift heavy ions, slow highly charged ions, nanostructures

Present Address:

e-mail: [elsaid@kfupm.edu.sa](mailto:elsaid@kfupm.edu.sa), [a.s.elsaid@fzd.de](mailto:a.s.elsaid@fzd.de)

Physics Department, King Fahd University of Petroleum and Minerals,

Dhahran 31261, Saudi Arabia

## 1. INTRODUCTION

The investigation of interaction processes of energetic ions and solids yields not only interesting basic phenomena but also provides access to promising technological applications in various fields [1, 2]. As nanotechnological tool, both swift heavy ions (SHI) and slow highly charged ions (HCI) were successfully utilized in nanostructuring of different materials [3, 4]. The effect is mainly attributed to the strong electronic excitations created when SHI slow down (electronic energy loss) and when HCI deposit their potential energy around the impact site [5, 6]. HCI excite only a small surface volume within few nm<sup>2</sup>, quite in contrast to SHI that produce an extended trail of electronic excitations along their trajectory deep into the bulk of the target material [11-13]. Despite the large difference in kinetic energy between HCI (eV-keV) and SHI (MeV-GeV), the coupling of the ion-induced electronic excitations to the lattice atoms is based on a similar mechanism [7, 8]. To produce pronounced modifications such as, e.g., nanohillocks, the energy transferred to the lattice atoms should in both cases exceed a certain threshold [9, 10]. For SHI, the creation threshold as well as geometry and size of the nanostructures depend on the ion beam parameters and target material. Many experiments showed that insulators are in general more sensitive to SHI-induced damage than semiconductors, which in turn are more sensitive than conductors and superconductors [14-16]. HCI-induced surface modifications are less well investigated but research got inspired and is benefitting from the knowledge available for SHI research results. Several recent studies compared SHI and HCI induced modifications in different materials including mainly oxides (SiO<sub>2</sub> [17], Al<sub>2</sub>O<sub>3</sub> [18], SrTiO<sub>3</sub> [10] and LiNbO<sub>3</sub> [19]) showing that both type of ions can produce the same shape of surface structures (hillocks or craters) of even similar size in some cases.

Here, we present a study on SHI and HCI induced surface modifications in the wide-bandgap semiconductor gallium phosphide (GaP). Nowadays, wide-bandgap semiconductors attract great interest due to device application e.g. as light-emitting diodes (LEDs) or semiconductor lasers operating at room temperature and in the visible light region [20, 21]. GaP is in particular promising for photoelectric applications in the visible to ultraviolet spectral region [22, 23]. The selection of GaP as newly HCI-studied material as well as comparing its response to swift heavy ions and slow highly charged ions can considerably contribute to reach a better understanding of the mechanisms responsible for the induced nanostructures formation.

## 2. EXPERIMENTAL

For the experiments we used 0.5 mm thick epitaxial (epi)-polished GaP single crystals (from MTI corporation, USA) of size 10 mm × 10 mm. The irradiations with high-energy ions were performed at the 6-MV tandem accelerator of HZDR (Dresden, Germany) with 30 MeV  $I^{9+}$  ions and at the Universal Linear Accelerator (UNILAC) facility of GSI (Darmstadt, Germany) with equilibrium charge state  $^{197}\text{Au}$  ions of kinetic energy between 374 MeV and 2.2 GeV. The energy variation was obtained through decelerating the 2.2 GeV ions provided by the accelerator by covering different parts of the crystals with Al foils of different thicknesses. For slow highly charged ions (HCI), the samples were irradiated with 114 keV  $^{129}\text{Xe}^{Q+}$  ( $Q = 33$  to  $40$ ) from the Electron Beam Ion Trap (EBIT) facility of HZDR [24]. The ion beam parameters, including nuclear and electronic energy loss and ion range, as estimated by the SRIM-2010 code [25], are listed in Table. 1. This is taking into consideration that the secondary energy loss to the target electrons is not considered. The applied fluence of the gold, iodine and xenon ions were  $5 \times 10^9$ ,  $5 \times 10^{10}$  and  $\sim 10^9$  ion/cm<sup>2</sup>, respectively. All irradiations were performed at room temperature and under normal beam incidence. The irradiated

samples were investigated by scanning force microscopy (SFM). The microscope (Nanoscope III, Digital Instruments) was operated using tapping mode in air utilizing Nanosensors PPP-NCLR probe of tip radius less than 10 nm. The Nanotec Electronica SL WSxM software (version 5.0 Develop 6.4) was utilized for image processing and dimension analysis of the SFM topographic images [26]. Changes of dielectric properties of the irradiated samples were tested with a rotating-compensator ellipsometer M-2000FI from J.A. Woolam Co. and WVASE32 (version 3.778) software. The ellipsometric parameters  $\Psi$  (amplitude) and  $\Delta$  (polarization) were recorded in a range from 210 to 1680 nm at a fixed angle position of  $75^\circ$  with respect to the surface normal [27]. The extinction coefficient ( $k$ ) and refractive index ( $n$ ) were calculated as a function of wavelength, assuming a homogenous bulk material.

### 3. RESULTS AND DISCUSSION

The topographic images of all GaP samples irradiated with SHI at the UNILAC (Au ions of kinetic energies between 374 MeV and 2.2 GeV and  $(dE/dx)_e$  between 27.2 and 29.8 keV/nm) showed nanohillocks protruding from the surface (Figs. 1). The hillocks are shown in the images as bright spots. The average (estimated from ~ 50 hillocks) hillock width and height range from 25 to 30 nm and from 0.4 to 0.9 nm, respectively (see Table 1). The width of a hillock was determined by defining two opposite points representing the regions where a height profile line (Left and Right foot) through the hillock maximum merges with the undamaged surface plane [6]. The roughness of the pristine samples was estimated to be ~ 0.2 nm, as shown in Fig. 2. Therefore, it should be considered as the minimum detection limit for the hillocks height. In contrast to swift gold ions, the surface of GaP irradiated at the 6-MV tandem accelerator with 54 MeV iodine ( $(dE/dx)_e = 10.3$  keV/nm) did not show any topographic features (Fig. 3). The critical  $(dE/dx)_e$  for hillock creation in GaP is obviously between 10.3 and 27.2 keV/nm.

This was in agreement with the detected threshold for a similar material, namely GaN of  $(dE/dx)_e$  threshold between 22.8 and 28.3 keV/nm [28].

The hillocks produced in GaP are similar in shape to the ones created by SHI in ionic fluoride single crystals [29-32], but their height is smaller (note, the hillock width is difficult to compare, because it is affected by the radius of the used SFM tip). The threshold for hillocks creation in ionic fluorides is  $\sim 5$  keV/nm which is significantly smaller than for GaP. Both, the smaller hillock height and the larger threshold of GaP are a clear indication of its lower sensitivity to ion damage compared to ionic fluorides and to many of the investigated oxides [17-19]. The existence of larger threshold for track formation by SHI in GaP was also predicted by Kamarou et. al. [33].

In contrast to SHI, no noticeable topographic changes were observed after irradiation with 114 keV highly charged xenon ions ( $Xe^{Q+}$ ),  $Q=33-40$ . This was concluded from the SFM measurements of the irradiated samples, where the dominated features in the measured topographic micrographs are only the grooves caused by polishing, as shown in Fig. 4. For surface nanostructuring with HCI, the potential energy ( $E_{pot}$ ) plays a similar role as the electronic energy loss does for SHI [34-36]. The fact that none of the different charge states of the used HCI create hillocks gives evidence that the potential energy threshold is above 38.5 keV. This value is in agreement with the one observed for GaN [28], of the same material category, and much larger than the threshold of 14 keV for calcium fluoride, as the most studied material. However, this value is shifted to even lower value  $\sim 12$  keV for slower ions [37]. This velocity effect can be considered as a hint for using slower HCI in order to reduce the threshold potential energy for surface nanostructuring of GaP [38].

In addition to the observed surface modifications, we also noticed that irradiation with SHI resulted in a color change of the irradiated crystals. The effect was even more

pronounced for higher kinetic energies due to the larger range of the ions (see inset of Fig. 5a). It was also confirmed by measuring a higher extinction coefficient in the visible light region for the sample area that was exposed to 2.2 GeV Au compared to the one exposed to 374 MeV Au ions (see Fig. 5a). This difference can be ascribed to the creation of more defects after irradiation with 2.2 GeV Au of mean energy loss ( $\langle dE/dx \rangle = 27.8$  keV/nm), than for 374 MeV of  $\langle dE/dx \rangle = 24.0$  keV/nm. This is taking into consideration that the mean energy loss was estimated for the ellipsometric-probed irradiated layer ( $\sim 4$   $\mu\text{m}$ ), i.e.  $\langle dE/dx \rangle = (E(\text{initial}) - E(\text{at } 4 \mu\text{m depth}))/4 \mu\text{m}$ , which was required in order to compare the damage induced by different kinetic energies. It is worthwhile mentioning that the presence of enough free carriers can cause also absorption of light, which termed free carrier absorption, at longer wavelength (usually infrared region) [39]. However, this effect was not observed in the irradiated GaP. In addition, in the UV region we observed smaller refractive indices for the 2.2 GeV Au irradiated samples than for the one irradiated with 374 MeV Au. In the visible and infrared spectral regions, no changes occur. This fact suggests that GaP has more attenuation and/ or refraction for the UV light, of higher energy, than the one for visible and infrared exhibiting lower energy.

#### 4. CONCLUSIONS

We have demonstrated that the interaction between SHI and GaP surface can result in the creation of surface nanohillocks. These nanostructures were not observed after irradiation with 54 MeV I ions of  $(dE/dx)_e = 10$  keV. Therefore, it was concluded that GaP requires a higher energy loss threshold between 10.3 and 27 keV/nm. However, by comparing similar material e.g. GaN, the lower limit can be shifted to  $\sim 20$  keV/nm [28]. Such nanostructures could not be also achieved by irradiation with 114 keV HCl even when using the highest available charge state (40+) of potential energy 38.5 keV.

Ellipsometry measurements for GaP irradiated with swift gold ions showed an increase of the extinction coefficients in the visible spectral regions for the ions exhibiting higher mean energy loss. Similarly, but in the UV spectral region, an increase of the refractive index was observed after irradiation with ions of higher mean energy loss.

#### ACKNOWLEDGEMENTS

Financial support by KFUPM (Projects: FT131018 and RG1326) is greatly acknowledged.

#### REFERENCES

- [1] C. L. Tracy, M. Lang, J. M. Pray, F. Zhang, D. Popov, C. Park, C. Trautmann, M. Bender, D. Severin, V. A. Skuratov, R. C. Ewing, *Nat. Commun.* 6, 6133 (2015).
- [2] F. Röder, G. Hlawacek, S. Wintz, R. Hübner, L. Bischoff, H. Lichte, K. Potzger, J. Lindner, J. Fassbender, R. Bali, *Scientific Reports* 5, 6786 (2015).
- [3] O. Ochedowski, O. Lehtinen, U. Kaiser, A. Turchanin, B. Ban-d'Etat, H. Lebius, M. Karlusic, M. Jaksic, M. Schleberger, *Nanotechnology* 26, 465302 (2015).
- [4] A. S. El-Said, W. M. Moslem, M. Djebli, *Appl. Phys. Lett.* 104, 231609 (2014).
- [5] R. A. Wilhelm, E. Gruber, R. Ritter, R. Heller, S. Facsko, F. Aumayr, *Phys. Rev. Lett.* 112, 153201 (2014).
- [6] A. S. El-Said, R. Neumann, K. Schwartz, C. Trautmann, *Surf. and Coat. Technol.* 158, 522 (2002).
- [7] F. Aumayr, S. Facsko, A. S. El-Said, C. Trautmann and M. Schleberger, *J. Phys.: Condens. Matter* 23, 393001 (2011).
- [8] R. A. Wilhelm, A. S. El-Said, F. Krok, R. Heller, E. Gruber, F. Aumayr, S. Facsko, *Prog. Surf. Sci.* 90, 377 (2015).
- [9] R. Heller, S. Facsko, R. A. Wilhelm, and W. Möller, *Phys. Rev. Lett.* 101, 096102 (2009).

- [10] A. S. El-Said, R. A. Wilhelm, R. Heller, S. Facsko, F. Aumayr, C. Trautmann, Nucl. Instr. Meth. B 269, 1234 (2011).
- [11] R. E. Lake, J. M. Pomeroy, H. Grube, C. E. Sosolik, Phys. Rev. Lett. 107, 063202 (2011).
- [12] A. S. El-Said, W. Meissl, M. Simon, J. R. Crespo López-Urrutia, I. C. Gebeshuber, J. Laimer, H. P. Winter, J. Ullrich, F. Aumayr, Rad. Eff. and Def. in Sol. 162, 467 (2007).
- [13] K. Schwartz, C. Trautmann, A. S. El-Said, R. Neumann, M. Toulemonde, W. Knolle, Phys. Rev. B 70, 184104 (2004).
- [14] C. Dufour, A. Audouard, F. Beuneu, J. Dural, J.P. Girard, A. Hairie, M. Levalois, E. Paumier, M. Toulemonde, J. Phys. Condens. Matter 5, 4573(1993).
- [15] Z. G. Wang, C. Dufour, E. Paumier, M. Toulemonde, J. Phys. Condens. Matter 6, 6733 (1995).
- [16] F. Masee, P. O. Sprau, Y. Wang, J. C. Séamus Davis, G. Ghigo, G. D. Gu, W. Kwok, Science Advances 1, e1500033 (2015).
- [17] A. S. El-Said, Nucl. Instr. and Meth. B **282**, 63 (2012).
- [18] N. Khalfaoui, J. P. Stoquert, F. Haas, C. Traumann, A. Meftah, M. Toulemonde, Nucl. Instr. Meth. B 268, 247 (2012).
- [19] A. S. El-Said, R. A. Wilhelm, S. Facsko, C. Trautmann, Nucl. Instr. Meth. B 315, 265 (2013).
- [20] H. Harima, J. Phys. Condens. Matter 16, S5653 (2004).
- [21] J. Václavík, D. Vápenka, EPJ Web of Conferences 48, 00028 (2013).
- [22] F. Hatami, V. Lordi, and J. S. Harris, H. Kostial, W. T. Masselink, J. Appl. Phys. 97, 096106 (2005).

- [23] G. Éthier-Majcher, P. St-Jean, A. Bergeron, A.-L. Phaneuf- L'Heureux, S. Roorda, S. Francoeur, *J. Appl. Phys.* 114, 034307 (2013).
- [24] U. Kentsch, G. Zschornack, F. Grossmann, V. P. Oysyanniko, F. Ulmann, *Hyperfine Interactions* 146-147, 237 (2003).
- [25] J. F. Ziegler, J. P. Biersack, and U. Littmark, *The Stopping and Range of Ions in Matter* (Pergamon Press, New York, 1985).
- [26] I. Horcas, et al. *Rev. Sci. Instr.* **78**, 013705 (2007).
- [27] Z. Qi-Xian, W. Wen-Sheng, R. Fang-Ping, *Chin. Phys. B* 20, 047802 (2011).
- [28] M Karlušić, et. al *J. Phys. D* 48, 325304 (2015)
- [29] C. Müller, M. Cranney, A. El-Said, N. Ishikawa, A. Iwase, M. Lang, R. Neumann, *Nucl. Instr. and Meth. B* 191, 246 (2002).
- [30] A. S. El-Said, M. Cranney, N. Ishikawa, A. Iwase, R. Neumann, K. Schwartz, M. Toulemonde, C. Trautmann, *Nucl. Instr. and Meth. B* 218, 492 (2004).
- [31] M. Toulemonde, A. Benyagoub, C. Trautmann, N. Khalfaoui, M. Boccanfuso, C. Dufour, F. Gourbilleau, J. J. Grob, J. P. Stoquert, J. M. Costantini, F. Haas, E. Jacquet, K.-O. Voss, and A. Meftah, *Phys. Rev. B* 87, 056102 (2013).
- [32] A. S. El-Said, R. Neumann, K. Schwartz, C. Trautmann, *Rad. Eff. and Def. Solids* 157, 649 (2002).
- [33] A. Kamarou, W. Wesch, E. Wendler, A. Undisz, and M. Rettenmayr. *Phys. Rev. B* 78, 054111 (2008).
- [34] G. Wachter, et al., *J. Phys. Conf. Ser.* 488, 132015 (2014).
- [35] R. Ritter, et al., *EPL*, 97, 13001 (2012).
- [36] C. Lemell, et al., *Solid-state electronics* 51,1398 (2007).
- [37] A. S. El-Said, R. Heller, R. A. Wilhelm, S. Facsko, F. Aumayr, *Appl. Surf. Sci.* 310,169 (2014).

[38] J. Hopster, R. Kozubek, B. Ban-d'Etat, S. Guillous, H. Lebius, M. Schleberger, 2D Materials 1, 1011011 (2014).

[39] D. Wiley and M. DiDomenico, Jr, Phys. Rev. B, 1, 1655 (1970).

### Figure Captions

Fig. 1. SFM topographic images ( $400 \times 400 \text{ nm}^2$ ) of GaP surface irradiated with  $5 \times 10^9 \text{ cm}^{-2}$  swift Au ions of various kinetic energies. The total kinetic energy and electronic energy loss is shown in each case.

Fig. 2. SFM topographic image ( $400 \times 400 \text{ nm}^2$ ) of GaP non-irradiated surface. The direction of fast scanning was from top to bottom. The graph shows line profile across the whole image.

Fig. 3. SFM topographic image ( $400 \times 400 \text{ nm}^2$ ) of GaP surface irradiated with  $5 \times 10^{10} \text{ cm}^{-2}$  54 MeV I ions. The electronic energy loss is shown.

Fig. 4. SFM topographic images ( $1.0 \mu\text{m} \times 1.0 \mu\text{m}$ ) of GaP surface irradiated with  $10^9 \text{ cm}^{-2}$  114 keV Xe highly charged ions of charge state  $Q= 36+$ ,  $38+$ , and  $40+$  corresponding to potential energy of 27.8, 33.0 and 38.5 keV, respectively.

Fig. 5. Spectroscopic ellipsometry of GaP crystals irradiated with  $5 \times 10^9 \text{ cm}^{-2}$  of 374 MeV (red) and 2.2 GeV (black)  $^{197}\text{Au}$  ions: (a) Extinction coefficient and (b) refractive index as a function of wavelength. The inset in (a) shows a photo of the sample illustrating the coloring effect of the ion beam.

Table 1. Ion beam parameters used for irradiation of GaP: potential energy  $E_{\text{pot}}$ , kinetic energy  $E_{\text{kin}}$ , electronic energy loss  $dE/dx_e$ , nuclear energy loss  $dE/dx_n$ , mean ion range  $R$  (calculated using SRIM-2010), and experimentally determined mean width ( $D$ ) and height ( $H$ ) of the created nanohillocks.

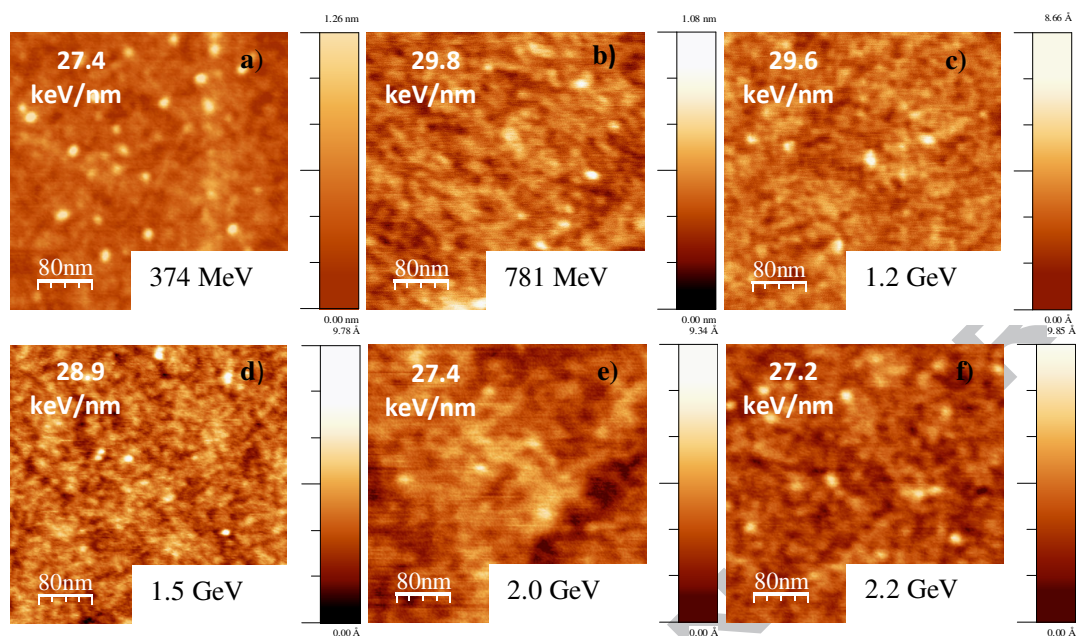


Figure 1: SFM topographic images ( $400 \times 400 \text{ nm}^2$ ) of GaP surface irradiated with  $5 \times 10^9 \text{ cm}^{-2}$  swift Au ions of various kinetic energies. The total kinetic energy and electronic energy loss are shown in each case.

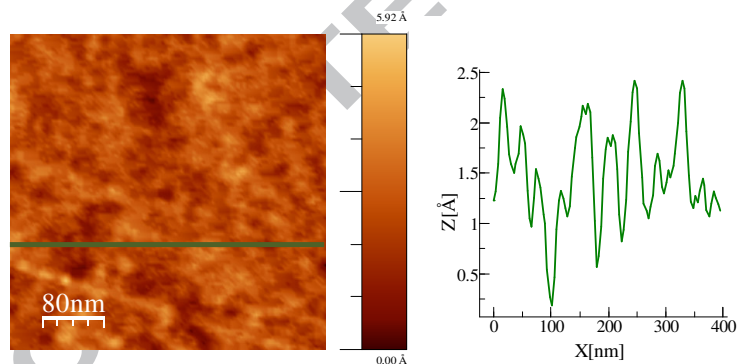


Figure 2: SFM topographic image ( $400 \times 400 \text{ nm}^2$ ) of GaP non-irradiated surface. The direction of fast scanning was from top to bottom. The graph shows line profile across the whole image.

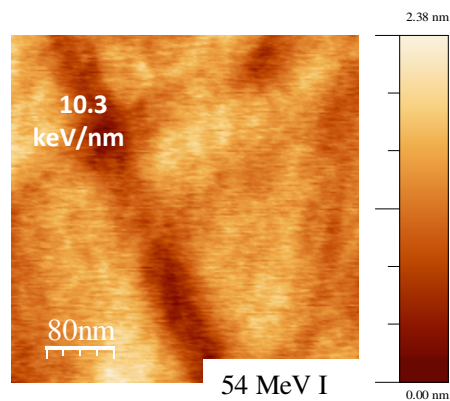


Figure 3: SFM topographic image ( $400 \times 400 \text{ nm}^2$ ) of GaP surface irradiated with  $5 \times 10^{10} \text{ cm}^{-2}$  54 MeV I ions. The electronic energy loss is shown.

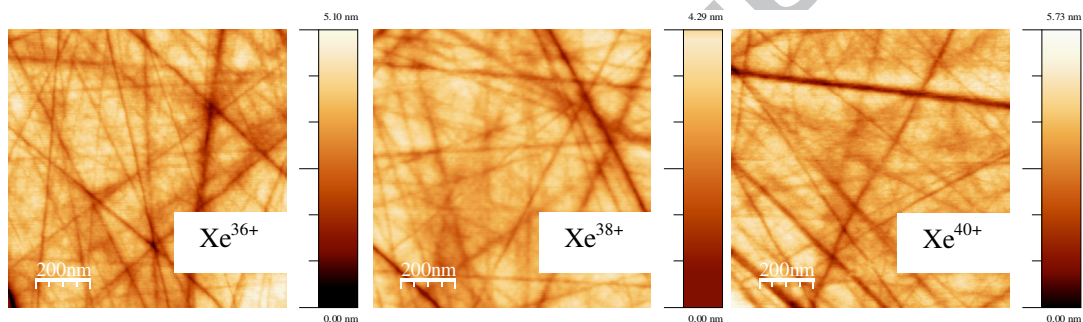


Figure 4: SFM topographic images ( $1.0 \mu\text{m} \times 1.0 \mu\text{m}$ ) of GaP surface irradiated with  $10^9 \text{ cm}^{-2}$  114 keV Xe highly charged ions of charge state  $Q=36+$ ,  $38+$ , and  $40+$  corresponding to potential energy of 27.8, 33.0 and 38.5 keV, respectively.

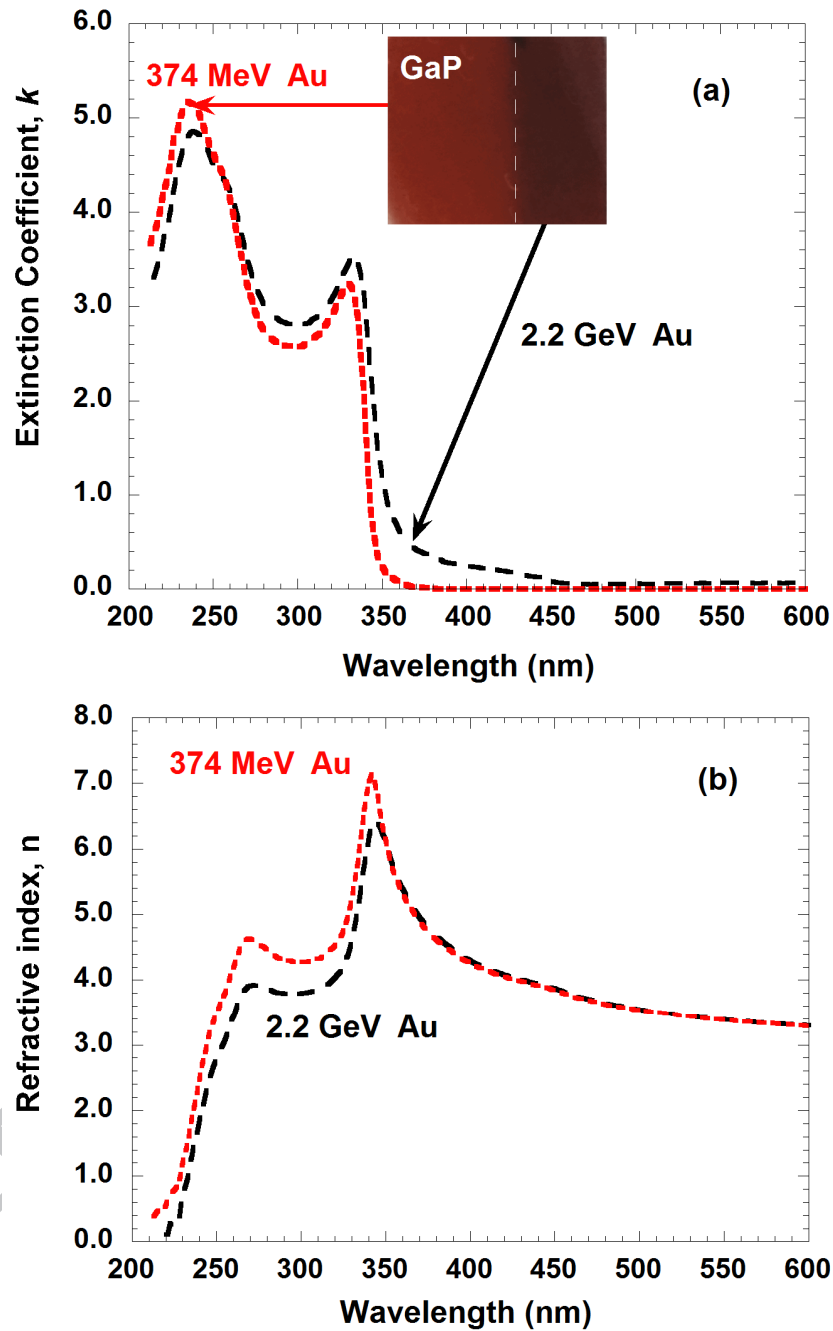


Figure 5: Spectroscopic ellipsometry of GaP crystals irradiated with  $5 \times 10^9 \text{ cm}^{-2}$  of 374 MeV (red) and 2.2 GeV (black)  $^{197}\text{Au}$  ions: (a) Extinction coefficient and (b) refractive index as a function of wavelength. The inset in (a) shows a photo of the sample illustrating the coloring effect of the ion beam.

**Table 1:** Ion beam parameters used for irradiation of GaP: potential energy  $E_{\text{pot}}$ , kinetic energy  $E_{\text{kin}}$ , electronic energy loss  $dE/dx_e$ , nuclear energy loss  $dE/dx_n$ , mean ion range  $R$  (calculated using SRIM-2010), and experimentally determined mean width ( $D$ ) and height ( $H$ ) of the created nanohillocks.

Ions	$E_{\text{pot}}$ keV)	$E_{\text{kin}}$	Degraded (Al) Thickness	$(dE/dx)_e$ keV/nm	$(dE/dx)_n$ keV/nm	Range	$D$ (nm)	$H$ (nm)
Xe <sup>33+</sup>	21.2	114 keV	-	0.3	2.75	13.8 nm	-	-
Xe <sup>36+</sup>	27.8	114 keV	-	0.3	2.75	13.8 nm	-	-
Xe <sup>38+</sup>	33.0	114 keV	-	0.3	2.75	13.8 nm	-	-
Xe <sup>40+</sup>	38.5	114 keV	-	0.3	2.75	13.8 nm	-	-
I <sup>9+</sup>	-	54 MeV	-	10.3	0.20	9.6 $\mu\text{m}$	-	-
Au <sup>25+</sup>	-	374 MeV	76 $\mu\text{m}$	27.4	0.13	24.5 $\mu\text{m}$	27.9 $\pm$ 3.1	0.9 $\pm$ 0.3
Au <sup>25+</sup>	-	781 MeV	61 $\mu\text{m}$	29.8	0.07	38.0 $\mu\text{m}$	29.8 $\pm$ 1.2	0.5 $\pm$ 0.3
Au <sup>25+</sup>	-	1.19 GeV	43 $\mu\text{m}$	29.6	0.05	51.5 $\mu\text{m}$	28.9 $\pm$ 3.3	0.4 $\pm$ 0.1
Au <sup>25+</sup>	-	1.48 GeV	31 $\mu\text{m}$	28.9	0.04	61.7 $\mu\text{m}$	25.6 $\pm$ 3.8	0.7 $\pm$ 0.1
Au <sup>25+</sup>	-	2.08 GeV	12 $\mu\text{m}$	27.4	0.03	83.0 $\mu\text{m}$	30.1 $\pm$ 3.6	0.4 $\pm$ 0.1
Au <sup>25+</sup>	-	2.19 GeV	-	27.2	0.03	86.9 $\mu\text{m}$	26.0 $\pm$ 5.0	0.4 $\pm$ 0.2